Quantifying the Role of Transport by Acoustic Streaming in MHz Focused-Ultrasound-Based Surface Sampling

Sillanpää, Tom Oskar Nikolai

IEEE
2022-12-01

Sillanpää , T O N , Mäkinen , J M K , Holmström , A , Pudas , T M , Hyvönen , J T J , Lassila , P J , Kuronen , A , Kotiaho , T , Salmi , A & Haeggström , E 2022 , Quantifying the Role of Transport by Acoustic Streaming in MHz Focused-Ultrasound-Based Surface Sampling . in 2022 IEEE International Ultrasonics Symposium (IUS) . IEEE , pp. 1-4 , 2022 IEEE International Ultrasonics Symposium (IUS) , Venice , Italy , 10/10/2022 . https://doi.org/10.1109/IUS54386.2022.995

http://hdl.handle.net/10138/355161
https://doi.org/10.1109/IUS54386.2022.9957858

submittedVersion

Quantifying the role of transport by acoustic streaming in MHz focused-ultrasound-based surface sampling

Tom Sillanpää
Electronics Research Laboratory,
Dept. of Physics and
Faculty of Pharmacy
University of Helsinki
Helsinki, Finland
tom.sillanpaa@helsinki.fi

Joni Mäkinen
Electronics Research Laboratory,
Dept. of Physics
University of Helsinki
Helsinki, Finland
joni.mk.makinen@helsinki.fi

Axi Holmström
Electronics Research Laboratory,
Dept. of Physics
University of Helsinki
Helsinki, Finland
axi.holmstrom@helsinki.fi

Topi Pudas
Electronics Research Laboratory,
Dept. of Physics
University of Helsinki
Helsinki, Finland
topi.pudas@helsinki.fi

Jere Hyvönen
Electronics Research Laboratory,
Dept. of Physics
University of Helsinki
Helsinki, Finland
jere.hyvonen@helsinki.fi

Petri Lassila
Electronics Research Laboratory,
Dept. of Physics
University of Helsinki
Helsinki, Finland
petri.j.lassila@helsinki.fi

Antti Kuronen
Dept. of Physics
University of Helsinki
Helsinki, Finland
antti.kuronen@helsinki.fi

Tapio Kotiaho
Faculty of Pharmacy and
Dept. of Chemistry
University of Helsinki
Helsinki, Finland
tapio.kotiaho@helsinki.fi

Ari Salmi
Electronics Research Laboratory,
Dept. of Physics
University of Helsinki
Helsinki, Finland
ari.salmi@helsinki.fi

Edward Hæggström
Electronics Research Laboratory,
Dept. of Physics
University of Helsinki
Helsinki, Finland
edward.haeggstrom@helsinki.fi

***Abstract*— We have developed an ultrasound-based surface sampling method permitting surface studies for liquid immersed samples. The method employs high-intensity focused ultrasound, which can remove material from predetermined areas and induce acoustic streaming that causes the immersion liquid to flow. In this study, we studied several conditions of acoustic streaming, which can affect particle transport away from the sampled surface. First, we explored suitable acoustic streaming conditions by finite element modelling. Next, we measured the induced streaming fields by particle image velocimetry. This study comprised cases, when a high-intensity focused ultrasound beam encountered a solid surface at different transducer-surface distances. A change in direction of streaming occurred when a focusing transducer was moved from 2λ defocus to 4λ defocus (towards the surface). Thus, we found suitable conditions for an upwards directing acoustic streaming field. This kind of defocus condition can be coupled to the surface sampling process allowing efficient particle transport for subsequent chemical analysis.**

Keywords—Acoustic streaming, surface sampling, FEM, MHz high-intensity focused ultrasound

INTRODUCTION

High-power ultrasound has proven useful for extracting material from various samples. For instance, ultrasound-assisted extraction (UAE) is used for rapid extraction of analytes e.g., from biological samples [1]. High-power ultrasonics at kHz frequency using ultrasound homogenizers is commonly applied in UAE. By using a tapered ultrasound horn-structure, the homogenizers can achieve more localized extraction or enables reduction of solvent volumes of the sonication bath. However, the horn-structure and the use of kHz-range ultrasound is not feasible for ultrasound imaging. For high-resolution imaging, MHz focused ultrasound (FUS) is required. FUS can be generated by e.g. for example, by a concave focusing piezo-element or a phased array.

Nonlinear acoustic phenomena, such as cavitation [2] and acoustic streaming [3]–[5], are observed when employing high-intensity ultrasound (HIFU) in liquid media. Sufficient peak-negative pressures induce transient cavitation that can cause erosion of the surface on which the HIFU beam is being focused by micro-jetting, microstreaming, and shock waves to detach material from a surface [6]. While the high-amplitude pressure waves propagate, the acoustic energy is absorbed by the medium and will induce Stuart-type acoustic streaming. It is worth noting that Stuart-type streaming will occur already at pressures lower than those required for cavitation.

When applying such HIFU beam, the induced acoustic streaming field is sensitive to exact boundary conditions of the system. Acoustic streaming is modulated e.g. by the amplitude and frequency of the waves, and the excitation mode of the transducer - pulsed or continuous wave mode. The boundary conditions can also be changed by interfaces placed in or near the propagation path.

Both phenomena, cavitation and acoustic streaming, have been employed in a HIFU-based surface sampling method that was developed for mapping the chemical composition of a sample surface [7]. The amplitude level of the HIFU beam needed for cavitation generation simultaneously induces acoustic streaming, which leads to the transfer of detached

particulates away from the surface. During sampling, the detached particulates can be captured into a sampling capillary from the liquid with a secondary liquid flow, applied by an external suction pump. The captured particulates are then transferred to subsequent chemical analysis, e.g. by mass spectrometry (MS). Depending on the sampling conditions, especially the transducer-sample distance, the sampling can either complement or compete against the suction flow. This study aims to quantify the role of acoustic streaming and explore suitable conditions for streaming to increase the particle transport towards the sampling capillary.

MATERIALS AND METHODS

Experimental Setup

The experimental setup is shown in Fig. 1A. We used a focusing transducer with a bowl-shaped piezo-crystal (Meggitt A/S, Kvistgaard, Denmark, Pz26, f = 7 MHz, OD = 22 mm, ID = 8 mm, R = 17 mm). Sinusoidal bursts (40 cycles/burst, pulse repetition frequency PRF = 2 kHz, duty cycle DC = 1.1 %) were generated with an arbitrary waveform generator (AFG31052, Tektronix, Oregon, USA). A power amplifier (500A100A, Amplifier Research, Pennsylvania, USA) was used to amplify the excitation signals. To align the HIFU beam, low amplitude waves were used, and the backscattered echoes from the reflector surface (aluminium plate) were monitored with an oscilloscope (5442D, Pico Technology, Cambridgeshire, UK) through a 10X attenuating probe (TA375, Pico Technology, Cambridgeshire, UK). The focus ($Z = F$) was determined by obtaining the highest echo amplitude from the surface, see Fig. 1B. 3D-translation stages with stepper motors were used to control the positioning of the transducer. The immersion bath was ultrapure water from a Milli-Q purification system (Millipore, Molsheim, France).

The acoustic and streaming fields were captured with a Schlieren imaging setup [8], which was complemented by a light-sheet for particle image velocimetry (PIV). The number density of tracer particles (polyethylene (PE) microspheres, ρ = 1 g/cm^3, D = (10-45) µm, Cospheric, California, USA) was 3100 particles/cm^3 (assuming 27.5 µm diameter spheres in the calculation of number of particles in the weighed mass of particle powder). The tracer particles that moved at a cross-section (slicing through the center of HIFU beam) were illuminated with the light-sheet. The light was emitted from a white-color high-power LED source described in [9] and the light-sheet was formed using a plano-convex cylindrical lens (LJ1075L2-A, Thorlabs, Newton, MA) and an adjustable line slit. The frame rate of video captures was 32 fps (time step = 31 ms between each frame). Measurements were performed at room temperature. A syringe pump (Nanojet, Chemyx, Stafford, USA) was used for suction flow.

Excitation voltages were converted to pressure values with a calibration measurement. The acoustic pressure as a function of excitation voltage (1 – 9 V) was measured at the focus of the transducer with a needle hydrophone (75 µm, NH0075, Precision Acoustics, UK). This voltage range was low enough to mitigate cavitation occurrence. By applying a linear fit to the data, the used excitation voltage (peak-positive voltage, u_{pp}, was 37.0 V) was converted to peak-positive pressure using the fitted parameter: $P_{PPP} = 0.53 \cdot u_{pp}$ (V) (R = 0.996), yielding P_{PPP} = 19.6 MPa.

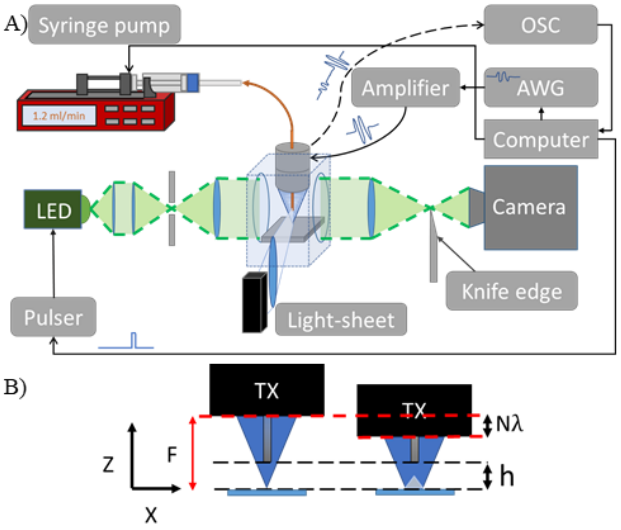

Fig. 1. A) *Schema of the Schlieren imaging setup used for PIV-measurements.* ***B)*** *Focusing scheme. F corresponds to distance, when the echo amplitude was at maximum, or R (geometric focus) in simulations.*

Finite Element Modelling

The experimental conditions were tested first by finite element modelling (FEM). Simulations were done with COMSOL Multiphysics® to study the acoustic streaming phenomenon. We explored suitable conditions to generate a streaming field that maximizes the transfer of material upwards from the analysis surface. Simulation conditions mimicked the experimental setup, using a 7 MHz transducer and water as the propagation medium.

To simulate the acoustic streaming, we used the standard perturbation approach [10]. First, the acoustic field was solved using COMSOL's *Thermoviscous Acoustics* module, which solves for the acoustic pressure (p_1) and velocity ($\vec{u}_1$). Then, the streaming field was solved using the *Laminar Flow* module such that a force term from the acoustic field was manually implemented into the flow equations. The following incompressible streaming equations were solved for:

$$(\vec{u}_2 \cdot \nabla)\vec{u}_2 = -\nabla p_2 + \mu\nabla^2\vec{u}_2 - \left\langle \frac{i2\pi f}{c_0^2} p_1 \vec{u}_1 \right\rangle - \langle \rho_0 (\vec{u}_1 \cdot \nabla)\vec{u}_1 \rangle$$

$$\rho_0 \nabla \cdot \vec{u}_2 = 0,$$

where $\vec{u}_2$ is the streaming velocity, p_2 is the streaming pressure, μ is viscosity, c_0 is the speed of sound and ρ_0 is the density. $\langle\cdot\rangle$ denotes time-averaging over the acoustic period. The last two terms on the right-hand-side are the force expressions from the acoustic field that drives the streaming.

The transducer was modelled as a pressure boundary condition (BC), p_1 = 30 kPa, which produced a pressure of ~2 MPa (including reflection) at the focus. To avoid a standing wave solution, we modelled a thin region near the transducer with the *Pressure Acoustic* module in COMSOL, utilizing a radiation BC with an incident pressure field. The bottom boundary was modelled as an impedance BC to mimic aluminium, along with a no-slip condition for the velocity field. The side boundaries of the geometry were modelled as impedance BC to match water and let acoustic energy out. For the streaming field, walls were modelled as no-slip and the side boundaries were set to be open boundaries. The opening

of the suction capillary was modelled as an outlet with a given flow rate.

In the simulations, the focus ($Z = R$) was determined as the geometrical focus of the focusing piezo-crystal. We performed the simulations at focus and at -6λ (= − 1.3 mm) defocus. The streaming fields were studied with and without the suction flow (1.2 ml/min).

Data Analysis

PIV-analysis was performed with PIVLab [11]. 200 frames were processed of each video capture. Pre-processing in PIV-analysis consisted of contrast limited adaptive histogram equalization (CLAHE) (window size 64 px) and high-pass filtering (60 px). Fast Fourier transformation (FFT) window deformation was used with the following interrogation area settings: first pass with area of 128 px (50 % overlap) and second pass with area of 64 px. The sub-pixel estimator was Gaussian 2x3-point, and a standard setting was chosen for correlation robustness. PIV-analysed frames were calibrated with a known reference distance (capillary width 192.92 px/1.58 mm) obtained from the images and for 31 ms time step.

Further data processing, e.g., median-filtering and plotting of images, were done with MATLAB. To visualize the acoustic field, the median of each pixel was determined from 10 Schlieren images. To visualize the particle trajectories, every 10th frame of 200 frames of the video recordings were superposed and some contrast enhancement was applied.

Results and Discussion

Results gained by FEM simulations for two different transducer-sample distances, at $Z = R$ and $Z = R - 6\lambda$, are shown in Fig. 2. The left-hand side of A and B display the acoustic pressure field in each condition, whereas the right-hand sides show the particle streaming velocity magnitude overlayed with flow vectors. The offset from $Z = R$ by -6λ showed a reversal in the direction of streaming along the center axis. Schlieren images in Fig. 3 display the acoustic field at both transducer-sample distances, agreeing with the simulated pressure field in Figs. 2A and 2B. The smooth gray rectangle in 3A and 3B is the sampling capillary, which was put close to the surface during the Schlieren captures.

Particle streaming trajectories at both transducer-sample distances, $Z = F$ and $Z = F - 6\lambda$ (with 1.2 ml/min suction flow), are visualized in Figs. 4A and B. The result from PIV-analysis for the video captures are shown in Fig. 4C and D. The particle streaming velocity component along the z-direction was plotted as a color map overlaid with streaming velocity vectors. At $Z = F$, the streaming mainly pointed downwards, with a minor contribution from the suction flow (Fig. 4C). By moving the transducer ($Z = F - 6\lambda$), the streaming pointed upwards, as predicted by simulations, see Fig. 2B.

The z-component of streaming velocities in different configurations, along a horizontal cross-section, are presented in Fig. 5. The horizontal cross-section was drawn through the maximum (upwards pointing stream) or the minimum (downwards pointing stream) of the streaming velocity, in the area between the sampling capillary and reflector surface. The z-component of particle streaming velocities were acquired in the following cases: 1) suction flow at rates: 0.6 and 1.2 ml/min, (Fig. 5A), 2) at transducer-sample distances $Z = F$ and $Z = F - 6\lambda$ with and without suction flow at flow rate

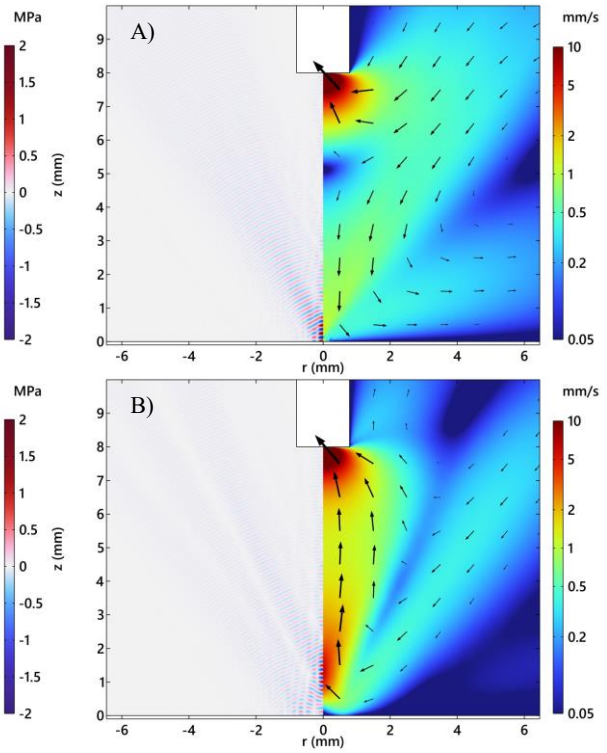

Fig. 2. A) *Acoustic pressure field and streaming field obtained by FEM at focus ($Z = R$) with the applied 1.2 ml/min suction flow.* ***B)*** *Simulated acoustic pressure field and streaming field at defocus ($Z = R - 6\lambda$) with the applied 1.2 ml/min suction flow. The color scale representing the magnitude of streaming velocity was plotted in logarithmic scale in* ***A)*** *and* ***B)*** *for better visualization.*

1.2 ml/min, (Fig. 5B). The offset in transducer-sample distance generated a suitable acoustic streaming flow from a surface sampling perspective.

Streaming fields acquired by measurements agreed with the fields predicted by FEM. However, the streaming along the transducer axis near the sampling surface, obtained from the PIV analysis, was unreliable. This could be attributed to several reasons, namely an insufficient tracer particle concentration for comprehensive PIV analysis, and strong acoustic radiation forces near the focus that impede particle movement.

We have noticed that particle streaming velocities as well as stream paths have size dependency. Especially the largest tracer particles (45 µm ≈ λ/5) were deflected by the acoustic radiation force, which could result in particles following the pressure field contours, or becoming trapped at pressure nodes. In contrast, the smaller particles easily moved along the

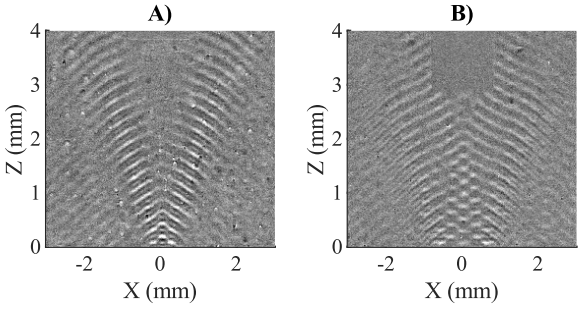

Fig. 3. A) *Schlieren image captured at the same transducer-sample distance as in Fig. 2A),* ***which displayed a similar reflected pressure field.*** ***B)*** *Schlieren image captured at the $Z = F - 6\lambda$ showing the focusing of waves between 1 and 2 mm above the reflector surface, agreeing with the simulated pressure field (Fig. 2B).*

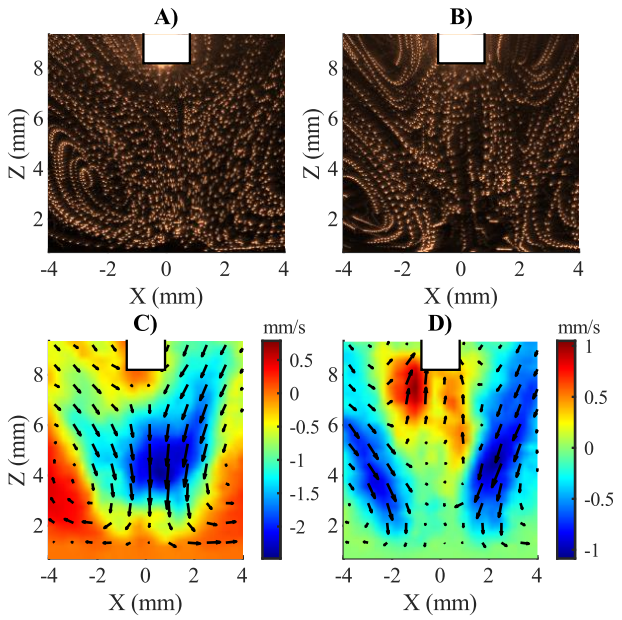

Fig. 4. *Tracer particle trajectories captured in the video recordings for PIV-analyses in the two cases:* ***A)*** $Z = F$ *and* ***B)*** $Z = F - 6\lambda$*. Every 10th frame of each video was summed on top of each other to generate the images in* ***A)*** *and* ***B)****.* ***C)*** *Measured streaming field with the same conditions as in 2A).* ***D)*** *Measured streaming field in the same conditions as in 2B). The change in the direction of acoustic streaming along the center axis was first predicted in simulations (2A) vs 2B)), later confirmed in measurements (4C vs 4D).*

streamlines of the induced streaming field. Hence, the PIV-analysis could be optimized for spatial resolution e.g. by using smaller tracer particles.

The transition from downwards to upwards acoustic streaming occurred between -2λ and -4λ defocus. The streaming velocity increased with the defocus distance, hence results from the -6λ defocus case were presented. Transducer

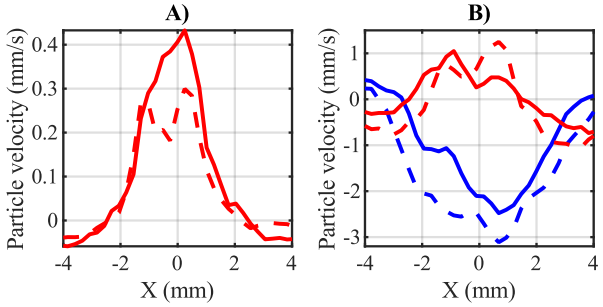

Fig. 5. A) *Line extraction of the w-component (z-direction) of particle streaming velocity below the sampling capillary at two suction flow rates: 0.6 and 1.2 ml/min.* ***B)*** *Line extraction of the w-component of particle streaming velocity below the sampling capillary at two Z distances (*$Z = F$ *and* $Z = F - 6\lambda$*). The suction flow (1.2 ml/min) had a minor effect on the particle streaming velocity. Dashed lines corresponded to cases without suction flow and solid lines with suction flow. Blue and cyan color depicts the downwards pointing particle streaming and red upwards.*

defocusing could be coupled to the surface sampling process. First a suitable streaming field could be generated at defocus, and subsequently the transducer would be moved to focus (or close to focus) and excited with high amplitude signals for material removal. Another possibility would be to apply the procedure in reverse. The method could benefit from two concentric piezo-crystals, one for generating streaming (being at defocus from the surface) and the other for removal (being focused on the surface).

CONCLUSIONS

Acoustic streaming plays an important role in the particle transport phenomenon of the HIFU-based surface sampling method. Particle streaming fields were modelled by FEM and characterized by particle image velocimetry. A suitable streaming condition, in which the particles stream upwards from the surface, was identified, which enhances mass transport away from the surface under HIFU treatment (e.g. sampling, cleaning, or machining).

REFERENCES

[1] F. Chemat, N. Rombaut, A.-G. Sicaire, A. Meullemiestre, A.-S. Fabiano-Tixier, and M. Abert-Vian, "Ultrasound assisted extraction of food and natural products. Mechanisms, techniques, combinations, protocols and applications. A review," *Ultrasonics Sonochemistry*, vol. 34, pp. 540–560, Jan. 2017, doi: 10.1016/j.ultsonch.2016.06.035.

[2] E. A. Neppiras, "Acoustic cavitation," *Phys. Rep.*, vol. 61, no. 3, pp. 159–251, May 1980, doi: 10.1016/0370-1573(80)90115-5.

[3] C. Eckart, "Vortices and Streams Caused by Sound Waves," *Phys. Rev.*, vol. 73, no. 1, pp. 68–76, Jan. 1948, doi: 10.1103/PhysRev.73.68.

[4] S. J. Lighthill, "Acoustic streaming," *J. Sound Vib.*, vol. 61, no. 3, pp. 391–418, Dec. 1978, doi: 10.1016/0022-460X(78)90388-7.

[5] Lord Rayleigh, "On the circulation of air observed in Kundt's tubes, and on some allied acoustical problems," *Philos. Trans. R. Soc. London*, vol. 175, pp. 1–21, 1884, doi: 10.1098/rstl.1884.0002.

[6] G. W. Gale and A. A. Busnaina, "Roles of Cavitation and Acoustic Streaming in Megasonic Cleaning," *Particulate Science and Technology*, vol. 17, no. 3, pp. 229–238, 1999, doi: 10.1080/02726359908906815.

[7] T. Sillanpää *et al.*, "Ultrasound-Based Surface Sampling in Immersion for Mass Spectrometry," *Unpublished*, 2022.

[8] E. Lampsijärvi, J. Heikkilä, I. Kassamakov, A. Salmi, and E. Hæggström, "Calibrated Quantitative Stroboscopic Schlieren Imaging of Ultrasound in Air," in *2019 IEEE International Ultrasonics Symposium (IUS)*, Oct. 2019, pp. 1651–1654. doi: 10.1109/ULTSYM.2019.8925916.

[9] C. Willert, B. Stasicki, J. Klinner, and S. Moessner, "Pulsed operation of high-power light emitting diodes for imaging flow velocimetry," *Meas. Sci. Technol.*, vol. 21, no. 7, p. 075402, Jun. 2010, doi: 10.1088/0957-0233/21/7/075402.

[10] P. B. Muller, R. Barnkob, M. J. H. Jensen, and H. Bruus, "A numerical study of microparticle acoustophoresis driven by acoustic radiation forces and streaming-induced drag forces," *Lab Chip*, vol. 12, no. 22, pp. 4617–4627, Oct. 2012, doi: 10.1039/C2LC40612H.

[11] W. Thielicke and R. Sonntag, "Particle Image Velocimetry for MATLAB: Accuracy and enhanced algorithms in PIVlab," *J. Open Res. Softw.*, vol. 9, no. 1, Art. no. 1, May 2021, doi: 10.5334/jors.334.